An Optimized Algorithm for InSAR Phase Unwrapping Based on Particle Filtering, Matrix Pencil, and Region-Growing Techniques

Juan J. Martinez-Espla, Tomas Martinez-Marin, and Juan M. Lopez-Sanchez, *Senior Member, IEEE*

***Abstract*—This letter presents a new phase unwrapping algorithm for synthetic aperture radar interferometry which combines a particle filter, a matrix-pencil (MP) local slope estimator, and an optimized region-growing technique. The advantages of the new method rely on the following contributions: The MP estimator provides better resolution to the local slope estimation, the particle filter enables simultaneous unwrapping and filtering without *a priori* statistics constraints, and the implemented region-growing technique adds diversity of unwrapping paths and ensures an optimum solution. Results introduced in this letter illustrate the main aspects of the new approach.**

***Index Terms*—Matrix pencil (MP), particle filter, phase unwrapping (PU), region growing, state space, synthetic aperture radar (SAR) interferometry.**

I. Introduction

In PREVIOUS works, the authors presented some phase-unwrapping (PU) algorithms based on the use of state-space techniques, such as the grid filter [1] and the particle filter [2]. The skeleton of these algorithms incorporates two main stages that are executed for every pixel. The first one, known as prediction stage, makes use of the previously unwrapped neighbors and the information provided by a local slope estimator to obtain a prediction for the unwrapped phase at a certain pixel. The second stage, known as update stage, incorporates the measurement (interferometric phase) at the pixel. Then, a filter combines prediction and measurement to obtain the optimal solution for that pixel, based on their covariance matrices, thus providing filtering and unwrapping simultaneously.

Regarding the filter, there are several options with different performances and different features from the view point of the state-space approach. For instance, an extended Kalman filter can be employed [3], and it propagates (i.e., maintains for future use for the rest of pixels) only the adopted solution state and the covariance matrix. In case of applying a particle filter [2], the algorithm maintains both the solution state and a selection from the rest of state candidates (also known as particles). This selection is performed by a third stage known as resampling, and only the states whose associated weights are the highest are maintained.

Manuscript received March 27, 2009; revised May 15, 2009. First published August 11, 2009; current version published October 14, 2009. This work was supported in part by the Spanish Ministry of Science and Innovation and in part by EU FEDER under Project TEC2008-06764-C02-02.

The authors are with the Departamento de Física, Ingeniería de Sistemas y Teoría de la Señal, Universidad de Alicante, 03080 Alicante, Spain (e-mail: jjme1@alu.ua.es; tomas@dfists.ua.es; juanma-lopez@ieee.org).

Digital Object Identifier 10.1109/LGRS.2009.2026496

Finally, a search strategy can be incorporated to add the capability of selecting the best pixel among all the candidates to be unwrapped at each time.

Among all the versions of the algorithm presented so far, the 2PFPU, which states for the monoseed path following version of the Particle Filter PU (PFPU), was demonstrated in [2] to be a very robust PU tool. This solution combines a particle filter, a local slope estimator based on the mode of the power spectral density (PSD) [3], and a monoseed path following search strategy [4].

In this letter, an improved PU solution is proposed. This solution also makes use of a particle filter, like the 2PFPU algorithm, but it incorporates two important differences which improve the overall performance of the approach. First, the local slope estimator based on the mode of the PSD has been replaced by a matrix pencil (MP) based one, since more accurate local phase slope predictions are expected from such a superresolution approach and smaller estimation windows can be employed. Second, an optimized region-growing strategy is used to drive the PU paths. As described later, the region-growing approach used here is optimum because only the pixel whose cost function is the best among all regions will be unwrapped at every step. The whole resulting method is more robust than previous ones because it can unwrap zones which other PU approaches simply mask or fail to unwrap, as illustrated in this letter with some examples.

This letter is organized as follows. Section II introduces the basics and advantages of using a particle filter for PU. Section III justifies the use of the MP-based local slope estimator. The optimized region-growing technique is presented in Section IV. Then, Section V illustrates the performance of the new method with some examples from both synthetic and real interferograms. Finally, conclusions are drawn in Section VI.

II. Particle Filtering

The particle filter was introduced in [2] to simultaneously perform filtering and PU. The Extended Kalman Filter introduced in [3] shares the same objective. However, the particle filter was shown to achieve better results than the Extended Kalman Filter since the latter is limited to Gaussian models, whereas the particle filter (PF) can model any kind of noise distributions. Note that the noise present in real interferograms is a marginal density distribution of the Wishart one.

A particle filter is a state-space algorithm, where each state has an associated weight indicating its importance among the complete space. Conceptually, the PF attempts to represent the posterior probability density function by a distribution of particles. The particles are defined as the set of states whose weights are the highest for each step. The objective is to calculate estimates of the states based on the set of all available observations up to current pixel.

Computationally, the PU algorithm based on a particle filter was shown to be an efficient solution since it can obtain accurate results but using only a selected group of states from the complete discrete space. In addition, it is also a precise method since the set of particles can be concentrated in the areas of interest.

III. MP-Based Local Slope Estimator

As it is well known, the precision of a local phase slope estimator based on the mode of the PSD is limited. This precision depends on the size of the window of data employed for the spectral (fast Fourier transform) estimation, which defines the sampling in the slope spectrum. A zero padding technique can be used to provide the slope estimations range with a higher granularity; however, it does not improve the precision of the estimator.

The MP technique belongs to a known group of super-resolution methods which do not suffer from this limitation. The basis for the calculus of certain parameters for sinusoids can be found in [5], and the idea and good performance of modeling a 1-D interferogram by a sum of dumped/undumped sinusoids was illustrated in [6]. However, we are interested in the calculus of bidimensional frequencies to model phase slopes at every pixel for bidimensional interferograms. Reference [7] provides a complete explanation on how to obtain bidimensional frequencies and, subsequently, the phase slope estimates. This reference constitutes the method implemented in the PU algorithm proposed in this letter.

IV. Optimized Region-Growing Technique

A. Introduction

The path following method used in [2] grows from a single seed or starting point of the interferogram, so it can be considered a monoseed region-growing technique. As a consequence, sometimes there will be no other chance than crossing an area with high density of residues, hence arising the risk of introducing unwrapping errors which could be propagated to the rest of the interferogram. Example B in Section V illustrates this effect. Contrarily, a higher number of seeds allows the unwrapping of good quality areas without having to cross bad quality ones until the end, thus obtaining more accurate results than a monoseed method.

Two different region-growing-based PU approaches have been developed for interferometric synthetic aperture radar (SAR) PU so far. The first one [8] is based on least squares methods and attempts to reach a global solution per region, merging the unwrapped regions afterward. In contrast, the region-growing technique introduced in [9] starts from different seeds and the corresponding areas grow simultaneously by following a pattern of thresholds. At every step, growth rings are defined and every candidate following the threshold criteria will be unwrapped. When no pixel is unwrapped at a step, the thresholds are relaxed and the process continues. As a result of the threshold scheme, this method is affected by two important drawbacks. First, it does not guarantee an optimal solution. Second, it is computationally inefficient.

The new region-growing algorithm presented in this letter is based on optimized search strategies [4]. The algorithm starts selecting an arbitrary number of seeds and creating their corresponding regions. Independently of the number of regions, pixels of the interferogram are only classified in two different sets. First, the set of unwrapped pixels with neighbors without unwrap, whose final weight distributions must be saved in order to be used to unwrap subsequent pixels [2]. Second, the set of wrapped pixels with unwrapped neighbors. The pixels of this last set, which represent the candidates to be unwrapped, will be ordered according to an associated cost function f_{c}. This cost function can be expressed as

$$f_{\mathrm{c}} = c_1 \cdot \mathrm{COH} + c_2 \cdot \mathrm{UNW} \tag{1}$$

where c_1 and c_2 are adjustable weights, COH represents the coherence of the pixel, and UNW the number of unwrapped neighbors. The slope estimation will be calculated as the average of the single slope estimations from the surrounding unwrapped neighbors [2]. Therefore, the higher UNW is, the better the cost function. Note that f_{c} is updated per step.

In this way, only the pixel whose cost function is the best will be unwrapped at every step, providing the optimal solution [4]. On the other hand, it is computationally efficient since it guarantees the unwrapping of one pixel per step.

The computational cost increase when compared to the monoseed algorithm is insignificant since pixels of the interferogram are only classified in two different sets, independently of the number of regions.

B. Merging Grown Regions

A key issue for the region-growing algorithm lies in solving the region collision problem. The solution described in [9] overlaps a group of pixels at once due to the method used to grow. For the PU algorithm proposed here, there will not be overlap between regions but a collision between adjacent pixels, one per growing region. This will simplify the solution as follows. Let us suppose there exists collision between regions 1 and 2. In such a case, a new region as the result of merging regions 1 and 2 will be created. Therefore, the discontinuity between both regions, which is a multiple of 2π, has to be removed. The unwrapped phase x^e_{1k} of pixel k in region 1 after removing this discontinuity can be obtained as

$$x^e_{1k} = x_{1k} + 2\pi m \tag{2}$$

where x_{1k} is the unwrapped phase at pixel k in region 1 still containing the discontinuity, and m is the ambiguity factor given by

$$m = \text{round}\left\{\frac{x_{2n} - x_{1k}}{2\pi}\right\} \tag{3}$$

being round$(\cdot)$ the nearest integer function, and x_{2n} the unwrapped phase at pixel n in region 2 (collision pixel at region 2).

C. Pseudocode of the Proposed PU Algorithm

The following steps define the overall proposed PU algorithm:

Step 1: A group of seeds is selected.
Step 2: Cost function f_c per seed is obtained.
REPEAT:
Step 3: The pixel contained in the set of wrapped pixels whose f_c is the highest will be unwrapped making use of the slope estimations from the surrounding unwrapped pixels and their weight distributions [2].
Step 4: IF region collision appears THEN solve the collision problem according to the method described in Section IV-B.
Step 5: Update lists of flags, weights, and cost functions f_c.
WHILE wrapped pixels remain.

V. Results

This section shows the results obtained when using the MP local slope estimator and the proposed PU algorithm. The first example (Example A) illustrates, both graphically and numerically, the more accurate predictions of the MP local slope estimator when compared against the local slope estimator based on the mode of the PSD. A comparison between a monoseed, or path following PU algorithm, and the proposed multiseed solution is also illustrated when dealing with low-quality areas, i.e., areas containing high concentration of residues (Example B). The better performance of the proposed multiseed PU algorithm is shown. This feature can be attributed to the diversity of growth paths used by the algorithm, which allows tackling difficult areas from different directions. Finally, the good results when unwrapping real interferograms by means of the proposed multiseed PU algorithm are also shown (Example C).

A. Local Phase Slope Estimates $\Delta\Phi$ for a Synthetic Cone

This example illustrates, both graphically and numerically, a comparison between slope estimates provided by the MP and the mode of the PSD. Fig. 1 shows a cone interferogram of size 100×100 pixels and 50 rad of height.

A graphical comparison between results obtained by both methods is shown in Fig. 2. The parameter shown in Fig. 2 is the slope in the horizontal direction, $\Delta\Phi_H$, computed by using a window of 3×3 pixels, for the complete cone interferogram

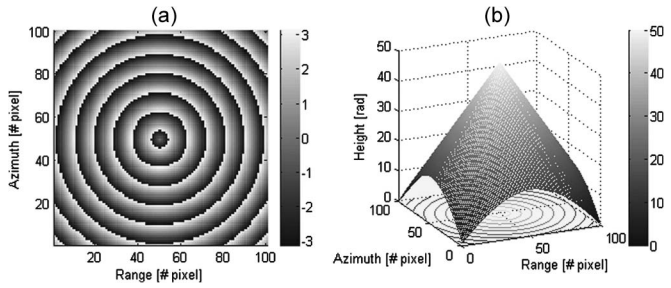

Fig. 1. Synthetic cone interferogram. (a) Input wrapped phase. (b) Expected unwrapped phase.

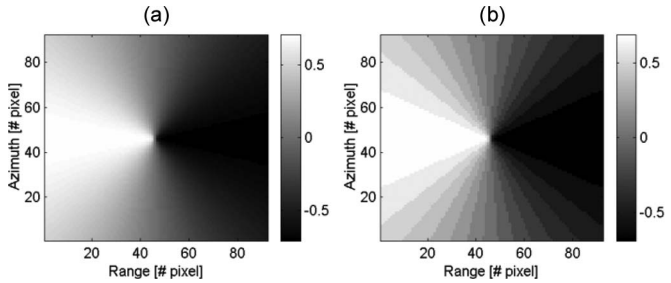

Fig. 2. Horizontal slope estimation $\Delta\Phi_H$ for the complete interferogram of Fig. 1, computed over with a 3×3 window by means of: (a) MP estimator and (b) mode of the PSD estimator.

TABLE I
SLOPE ESTIMATES CALCULATED AT PIXEL (30, 5): EXPECTED VALUES AND RESULTS OBTAINED BY MEANS OF BOTH THE MP AND THE MODE OF THE PDS LOCAL SLOPE ESTIMATORS

	Expected	MP	PSD_{mode}
$\Delta\Phi_H$ (rad/pixel)	*0.6450*	*0.6461*	*0.6872*
$\Delta\Phi_V$ (rad/pixel)	*0.2811*	*0.2872*	*0.2945*
$\Delta\Phi_{OH}$ (rad/pixel)	*0.9314*	*0.9332*	*0.9817*
$\Delta\Phi_{OV}$ (rad/pixel)	*0.3463*	*0.3590*	*0.3927*

in Fig. 1. The better precision of the MP estimator is clearly demonstrated by the smoother aspect of the image.

A numerical comparison between the slope estimators for a single pixel of the same synthetic cone interferogram, for instance pixel (30, 5), is shown in Table I. Slope estimates in horizontal ($0°$, $\Delta\Phi_H$), vertical ($90°$, $\Delta\Phi_V$), oblique-horizontal ($+45°$, $\Delta\Phi_{OH}$), and oblique-vertical ($-45°$, $\Delta\Phi_{OV}$) directions have been calculated from pixel (30, 5) to the surrounding ones with the same 3×3 window. The better precision of the MP estimator is clearly demonstrated by the values in this table.

B. Synthetic Pyramid Containing Two Very Noisy Strips

As introduced in Section IV-A, when a monoseed region growing or a conventional path following PU algorithm is used, sometimes there will be no other chance than crossing a low-quality or noisy area. It yields the risk of erroneous PU and its propagation to the remaining pixels. Instead, when the proposed multiseed algorithm is used, good quality areas are unwrapped first, and low-quality ones can be approached from different sides at once, thus increasing the chance of success. To illustrate this feature, an input pyramidal synthetic interferogram has been contaminated with two longitudinal strips of Wishart noise

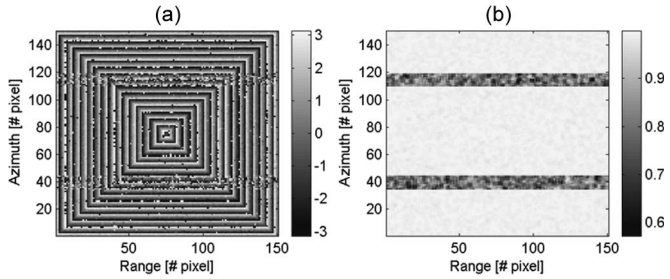

Fig. 3. Pyramidal interferogram containing two strips of Wishart noise. (a) Wrapped input signal. (b) Coherence.

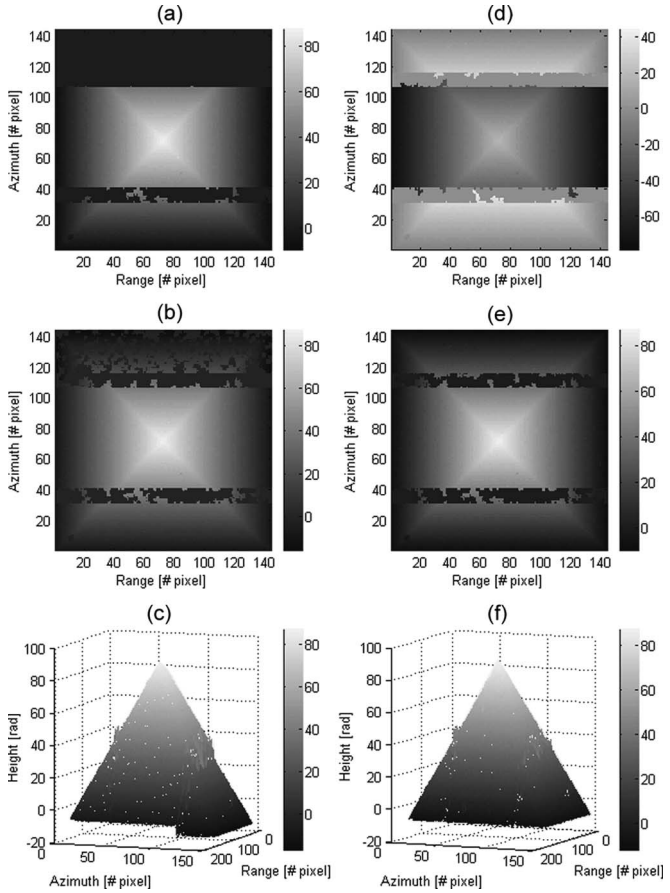

Fig. 4. Pyramidal interferogram containing two strips of Wishart noise. (a) Monoseed algorithm: result after 62.2% unwrapped pixels. (b) Monoseed algorithm: result after 75.5% unwrapped pixels. (c) Monoseed algorithm: final solution. (d) Multiseed algorithm: collision of regions 1 and 2. (e) Multiseed algorithm: collision of regions 2 and 3. (f) Multiseed algorithm: final solution.

[see Fig. 3(a)]. Fig. 3(b) shows the corresponding coherence of the data.

Fig. 4(a) and (b) shows intermediate results at two instants of the unwrapping process when a monoseed version of the proposed method is used. Then, Fig. 4(c) shows the erroneous final solution for this method. Fig. 4(d) and (e) shows intermediate results when the proposed multiseed algorithm is used instead, including the merging process between regions. It can be observed how the monoseed algorithm has no other chance that crossing both noisy strips from one side to the other. The low quality of the data inside the strips involves a low reliability of the slope predictions and the phases themselves, which has

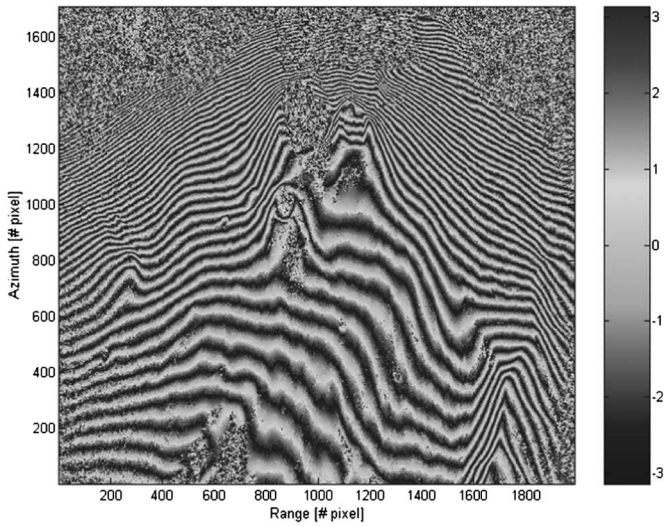

Fig. 5. Input phase of the X-SAR interferogram over Mount Etna.

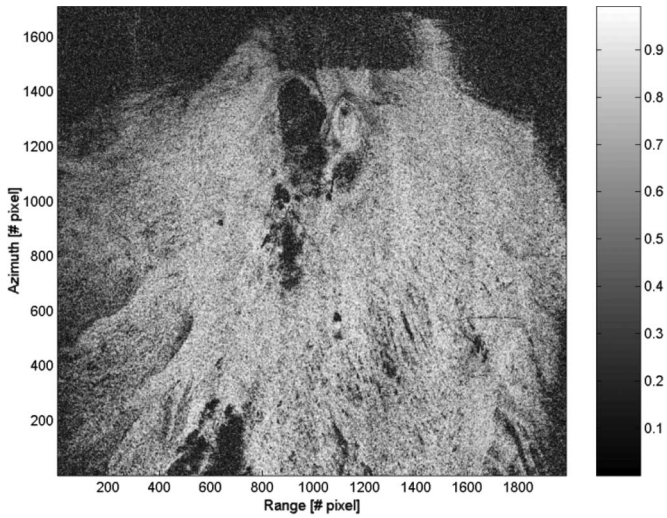

Fig. 6. Coherence of the X-SAR interferogram over Mount Etna.

dramatic consequences when crossing from one side to another. Unlike this, the proposed multiseed PU algorithm can unwrap before both high-quality regions independently. In this way, the low-quality strips can be approached from both high-quality sides at once, thus increasing the success chances. In fact, Fig. 4(f) shows the correct unwrapped phase when the proposed multiseed algorithm is used. Concerning the computational cost increase of the multiseed method, it was insignificant (only 1% higher) when compared to the monoseed method.

C. X-SAR Interferogram Over Mount Etna

The data shown in Figs. 5 and 6 are the input wrapped phase and the coherence, respectively, extracted from an interferogram formed by a pair of single look complex images with 1718 $\times$ 1992 pixels, acquired by the X-band SAR (X-SAR) mission over Mount Etna. The sea region (at the top) has been masked out since the phase information is meaningless in this area.

Fig. 7 shows the unwrapped phase by means of the proposed multiseed PU algorithm. A quality test of this solution is shown

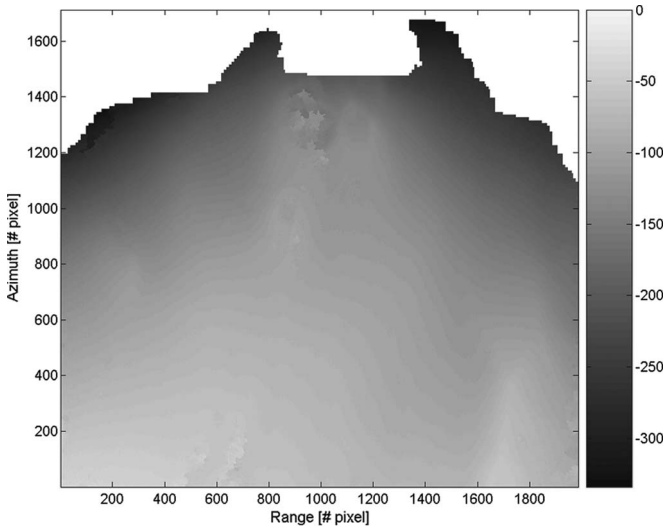

Fig. 7. Unwrapped phase by the multiseed algorithm for the X-SAR interferogram over Mount Etna. Implementation detail: The continuous space contained inside the 2π sliding window has been translated into a discrete state space composed of $N = 100$ cells and a maximum of $N_s = 50$ particles will be used (see [2] for cell and particle definitions).

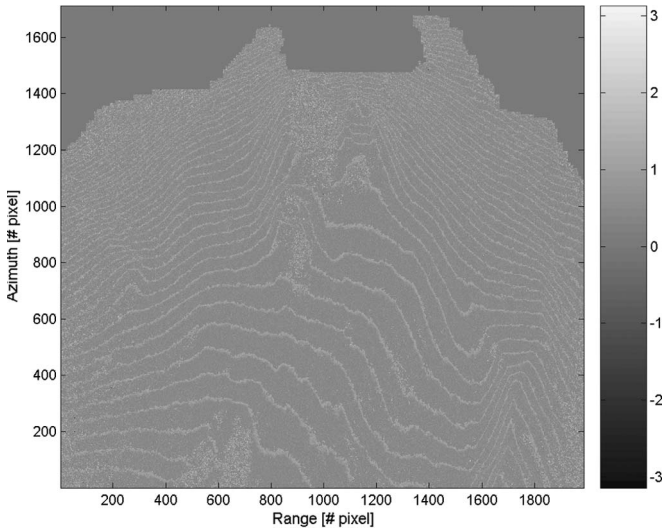

Fig. 8. Wrapped phase difference between the unwrapped phase (output of the proposed multiseed algorithm) and the input wrapped phase for the X-SAR interferogram over Mount Etna.

in Fig. 8, where, as expected, the wrapped phase difference between the solution and the original interferogram exhibits a noisy constant aspect, and no bias has appeared despite the big size of the interferogram. Note that thin lines of nonzero values appear in this figure located close to the transitions between fringes in the input phase. These lines are a consequence of the filtering capability incorporated by this method.

VI. Conclusion

A new method to simultaneously filter and unwrap the phase contained in a SAR interferogram is presented in this letter.

This solution combines a particle filter, a local slope estimator based on the MP technique introduced in [7], and an optimized version of the region-growing search strategy introduced in [9]. The better precision of the MP local slope estimator when compared to the one based on the mode of the PSD has been shown. A comparison between the proposed multiseed PU algorithm and its monoseed version has illustrated the better performance of the former when dealing with low-quality areas. Finally, the proposed PU algorithm has been applied to a real interferogram, showing a correct performance.

Our research line at present and in the near future is focused on the application of these state-space unwrapping strategies in advanced differential SAR interferometry for ground deformation monitoring, where the time coordinate has to be incorporated in the formulation.

Acknowledgment

The authors would like to thank Dr. K. P. Papathanassiou (Deutsches Zentrum für Luft- und Raumfahrt e.V.) and Dr. C. Lopez-Martinez (Universitat Politecnica de Catalunya) for providing access to the X-SAR images of Mount Etna.

References

[1] J. J. Martinez-Espla, T. Martinez-Marin, and J. M. Lopez-Sanchez, "Using a grid-based filter to solve InSAR phase unwrapping," *IEEE Geosci. Remote Sens. Lett.*, vol. 5, no. 2, pp. 147–151, Apr. 2008.

[2] J. J. Martinez-Espla, T. Martinez-Marin, and J. M. Lopez-Sanchez, "A particle filter approach for InSAR phase filtering and unwrapping," *IEEE Trans. Geosci. Remote Sens.*, vol. 47, no. 4, pp. 1197–1211, Apr. 2009.

[3] O. Loffeld, H. Nies, S. Knedlik, and W. Yu, "Phase unwrapping for SAR interferometry—A data fusion approach by Kalman filtering," *IEEE Trans. Geosci. Remote Sens.*, vol. 46, no. 1, pp. 47–58, Jan. 2008.

[4] N. J. Nilsson, *Artificial Intelligence: A New Synthesis*. San Mateo, CA: Morgan Kaufmann, 1998.

[5] Y. Hua and T. K. Sarkar, "Matrix pencil method for estimating parameters of exponentially damped/undamped sinusoids in noise," *IEEE Trans. Acoust., Speech, Signal Process.*, vol. 38, no. 5, pp. 814–824, May 1990.

[6] G. Nico and J. Fortuny, "Using the matrix pencil method to solve phase unwrapping," *IEEE Trans. Signal Process.*, vol. 51, no. 3, pp. 886–888, Mar. 2003.

[7] Y. Hua, "Estimating two-dimensional frequencies by matrix enhancement and matrix pencil," *IEEE Trans. Signal Process.*, vol. 40, no. 9, pp. 2267–2280, Sep. 1992.

[8] G. Fornaro and E. Sansosti, "A two-dimensional region growing least squares phase unwrapping algorithm for interferometric SAR processing," *IEEE Trans. Geosci. Remote Sens.*, vol. 37, no. 5, pp. 2215–2226, Sep. 1999.

[9] W. Xu and I. Cumming, "A region-growing algorithm for InSAR phase unwrapping," *IEEE Trans. Geosci. Remote Sens.*, vol. 37, no. 1, pp. 124–134, Jan. 1999.